A Modeling-Based Design to Engineering Protein Hydrogels with Random Copolymers

Terms of use:

(Article begins on next page)

25 April 2024

A Modeling-Based Design to Engineering Protein Hydrogels with Random Copolymers

Annalisa Cardellini,[†,‡] Felipe Jiménez-Ángeles,[‡] Pietro Asinari,[*,†,¶] and Monica Olvera de la Cruz[*,‡,§]

†*Politecnico di Torino, Torino, 10129 Italy*

‡*Department of Materials Science and Engineering, Northwestern University, Evanston, Illinois 60208, United States*

¶*Istituto Nazionale di Ricerca Metrologica, 10135 Torino, Italy*

§*Department of Chemistry, Northwestern University, Evanston, Illinois 60208, United States*

E-mail: pietro.asinari@polito.it; m-olvera@northwestern.edu

ABSTRACT

Protein enzymes have shown great potential in numerous technological applications. However, the design of supporting materials is needed to preserve protein functionality outside their native environment. Direct enzyme-polymer self-assembly offers a promising alternative to immobilize proteins in an aqueous solution, achieving higher control of their stability and enzymatic activity in industrial applications. Here, we propose a modeling-based design to engineering hydrogels of Cytochrome P450 and of PETase with styrene/2-vinylpyridine (2VP) random copolymers. By tuning the copolymer fraction of polar groups and of charged groups *via* quaternization of 2VP for co-assembly with Cytocrome P450 and *via* sulfonation of styrene for co-assembly with PETase, we provide quantitative guidelines to select either a protein-polymer hydrogel structure

or a single protein encapsulation. The results highlight that, regardless of the protein surface domains, the presence of polar interactions and hydration effects promote the formation of a more elongated enzyme-polymer complex, suggesting a membrane-like co-assembly. On the other hand, the effectiveness of a single protein encapsulation is reached by decreasing the fraction of polar groups and by increasing the charge fraction up to 25%. Our computational analysis demonstrates that the enzyme-polymer assemblies are first promoted by the hydrophobic interactions which lead the protein non-polar residues to achieve the maximum coverage and to play the role of the most robust contact points. The mechanisms of co-assembly are unveiled in the light of both protein and polymer physical-chemistry, providing bio-conjugate phase diagrams for the optimal material design.

KEYWORDS: hydrogels, protein encapsulation, cytochrome P450, PETase, random copolymers, enzyme-polymer assemblies

INTRODUCTION

Natural and synthetic enzymes have shown attractive prospects in a variety of engineering applications, defining frontiers in fuel catalysis,[1,2] pollutant reduction[3] as well as drug metabolization,[4] glucose detection, and biosensing.[5] The stability of proteins and their functionality are often compromised outside their natural environment leading to undesirable consequences in the process efficiency. Incompatible conditions such as high temperature, unfavorable pH, and the presence of organic solvents can easily result in the denaturation of enzyme structures, which often manifests as a decline in their activity. Preservation of proteins as gels has been known in food applications for long time.[6] Therefore, reversible aggregation and gelation of globular proteins has been widely studied using scattering methods and patchy models in coarse-grained molecular simulations.[7,8]

A variety of recent approaches have been identified to deliver proteins, to limit their denaturation, and to maintain their enzymatic activity, structural properties, and selectiv-

ity.[5,9-12] For example, covalent grafting of hydrophobic polymer moieties to proteins has introduced advantages to localize proteins, restrict their unfolding, and improve the stress resistance of materials.[13,14] A general polymerization method to synthesize protein-polymer bioconjugates from a biomacroinitiator (BSA-Br, Io) demonstrated that a photoinduced copper-mediated radical polymerization can maintain the secondary structure of Bovine Serum Albumin (BSA) protein.[14] Bioconjugates consisting of one globular protein block (mCherry) grafted to one polymeric chain can self-arrange in bulk[15-17] and can form thin film nanostructures,[18] thereby guaranteeing an efficient protein immobilization. Moreover, the shape-conformation of protein-polymer conjugates exhibit phase transitions from disordered to lamellar, hexagonal, and rod-like structures in diverse proteins.[19] The covalent grafting techniques, however, frequently need either the use of organic cosolvents which trigger the denaturation of proteins, or deoxygenation which is a high-cost and time-demanding process. As a result, the drawbacks of the grafting process have strongly restricted the preparation of protein-polymer bio-complexes on large scale.

Self-assembly of enzyme-polymer complexes exploits non-covalent interactions and is a promising method to preserve protein integrity. Beyond the effective simplification of the preparation process and the prevention of denaturation, the direct protein-polymer self-assembly provides significant flexibility and prompt responsiveness to external physical stimuli enabling a reversible behavior of the supramolecular complexes. In this direction, a macromolecular ferritin crystal with integrated hydrogel polymers was synthesized.[20] The resulting material manifests a notable elasticity while retaining the periodic order and facet morphology. Moreover, the expansion-contraction cycles and therefore the self-healing properties were tested on the hydrogel-based crystal by alternating the divalent and monovalent metal-salt solution. A multi-responsive complex composed of apoferritin and block copolymers which dynamically self-assemble by altering the temperature and electrolyte concentration of the solutions was developed.[21]

Within the prospect of direct enzyme-polymer non-covalent complexation, amphiphilic

heteropolymers offer a versatile approach for protein solubilization and stabilization. The capability to synthesize random heteropolymers with reliable control over the statistical monomer distribution affords promising developments towards a rational match between the surface patterns of natural proteins and polymer side chains. Successful results in this direction have been obtained by B. Panganiban and coworkers[11] who presented an efficient design approach of random heteropolymers based on protein surface patches while maintaining the enzymatic activity in a foreign environment. More recently, an experimental and modeling combined approach has been developed in our group to segregate organic molecules in water by using polyelectrolyte complexes composed of random copolymers.[22] Clearly, the chemical diversity of protein surface patterns and the experimental challenges of tailored polymer design often prevent the development of general and sustainable protocols for an effective protein co-assembly with random copolymers. Therefore, although some attempts have manifested promising scenarios, the prediction of the enzyme-random copolymer self-assembly conformation based on their physical-chemistry properties, remains a challenge. Indeed, to achieve protein co-assembly with random copolymers into various structures, from hydrogels to single protein encapsulation, the monomer chemical composition for specific protein surface domains are required, as well as understanding the cooperative interactions between the different chemical groups. Sophisticated computational algorithms have shown a great ability to fast classify the protein surface domains,[23–25] however, a synergistic and chemical precise analysis on the interactions among enzymes and polymers in an aqueous solution is still lacking, which is strongly suggested to address a more rational design of direct enzyme-random copolymer self-assembly.

In this article, the ability to co-assemble proteins with random copolymers in aqueous solutions is investigated by using a coarse-grained (CG) molecular dynamics approach.[26,27] Our modeling-based design is used on self-assemblies composed of polystyrene-based random copolymers and proteins, namely Cytochrome P450, which is negatively charged (-15e), and PETase which is instead positively charged (+6e). Cytochrome P450 is one of the most

versatile biocatalysts in nature, able to metabolized around 75 % of drugs.[28] P450s are crucial in a broad variety of chemical reactions particularly important for pharmaceuticals, terpenes, gaseous alkanes, and more.[29,30] On the other hand, PETase is an efficient poly(ethylene terephthalate) plastic-degrading enzyme.[31] Here, a thorough analysis on enzyme-polymer shape conformation is carried out to observe and quantify the effects of varying the polar (f_p) and charged (f_c) monomer fractions in the enzyme-polymer self-assembly, also known as bioconjugates (see Figure 1). Our simulations are performed using a cubic simulation box (of 20 nm per side) containing one protein enzyme, 20 polymer molecules, and the necessary water molecules to create an aqueous solution. The equivalent mass densities (6.52 g/L for the protein and 25.9 g/L for the polymers) are comparable to the experimental values in related protein-polymer hydrogels.[20] The macroscopic behavior is mimicked by imposing periodic boundary conditions in the three spatial directions. The dielectric changes and polarization effects play a key role in the adsorption of charged species at interfaces.[32,33] Hence, we use polarizable water particles[34] to account for the transition from high dielectric constant away from the proteins ($\varepsilon_w \approx 80$ in bulk water) to low dielectric permittivity near the proteins' surface. We show that the polarization effects indeed affect protein-polymer conformation.

The results, organized in phase diagrams, highlight the role of neutral hydrophilicity to obtain a membrane-like co-assembly in water, namely, a polymer-enzyme network cross-linked *via* specific and non-specific interactions. The co-assemblies forming an extended network are referred to as membrane-like structures or as hydrogels.[35] On the other hand, the increase of charged building blocks within the random copolymers enhances the formation of compact and wrapped bio-complexes, inhibiting the bio-assembly network. Beyond the advantages defined by the phase diagrams, and the capability of screening polymer compositions in a semi-quantitative fashion, our computational approach lightens the dominant physical-chemistry interactions driving the self-assembly mechanisms and the related protein encapsulation efficiency. In the method section, we describe both the main details about the

CG self-assembly simulations, and post-processing tools developed to explore the impact of nonbonded interactions while the self-assembly takes place.

RESULTS AND DISCUSSION

Coarse-Grained (CG) Model of Protein-Polymer Complexes

The enzyme-polymer complexation offers a promising strategy to encapsulate, immobilize, and delivery proteins in a wide range of applications. The study carried out here demonstrates the potential advantages of using coarse-grained molecular dynamics (CG-MD) simulations to engineer the design of protein assemblies with polystyrene-based random copolymers in water. Our results provide an efficient polymer composition screening according to the desired co-assembly mode required for a specific application.

The direct formation of enzyme-heteropolymer complexes is carried out in an aqueous solution at 1:20 protein-copolymers composition ratio. Because of their extremely high impact in the biological and energy fields, Cytochrome P450 (-15e) and PETase (+6e) proteins are selected and modeled with the standard Martini force field[26,36] as illustrated in Figure 1a. The heteropolymers are designed by randomly distributed hydrophobic (styrene (S)), polar (2-vinyl pyridine (2VP)), negative (styrene-sulfonate (SS)) and positive (quaternized-2-vinyl pyridine (Q-2VP)) charged monomers. Accordingly, we define f_p and f_c as the percentage of polar and charged monomers, respectively, within one single chain (Figure 1b)). To address a rational screening of heteropolymers, we tested many protein-polymer aqueous solutions by a systematic tuning of f_p and f_c parameters. Specifically, we explore: (i) a progressive increase, from 0 to 100%, of f_p by replacing styrene with neutral polar monomers in PS-2VP polymers; (ii) an enhancement, from 0 to 40%, of f_c by altering the fraction of Q2VP and SS monomers in polystyrene-based chains, (iii) a simultaneous increment of polar and charged fractions by randomly distributing 2VP and Q2VP monomers to form complexes with the negatively charged Cytochrome P450, and 2VP and SS to form PETase-based complexes

a Proteins

P450 protein

AA model   CG model

PETase protein

AA model   CG model

b Monomers

Styrene **(S)**

AA model   CG model

POLARITY

2-vinylpyridine **(2VP)**

AA model   CG model

CHARGE

CHARGE

Styrene sulfonate **(SS)**

AA model   CG model

Quaternized 2-vinylpyridine **(Q2VP)**

AA model   CG model

c Enzyme-polymer complexes

P450 { (i) PS-2VP
       (ii) PS-Q2VP
       (iii)PS-2VP-Q2VP

PETase { (i) PS-2VP
         (ii) PSS
         (iii)PSS-2VP

$N \rightarrow$ nr. of monomers

$$f_p = \frac{N_{polar}}{N_{tot}}$$

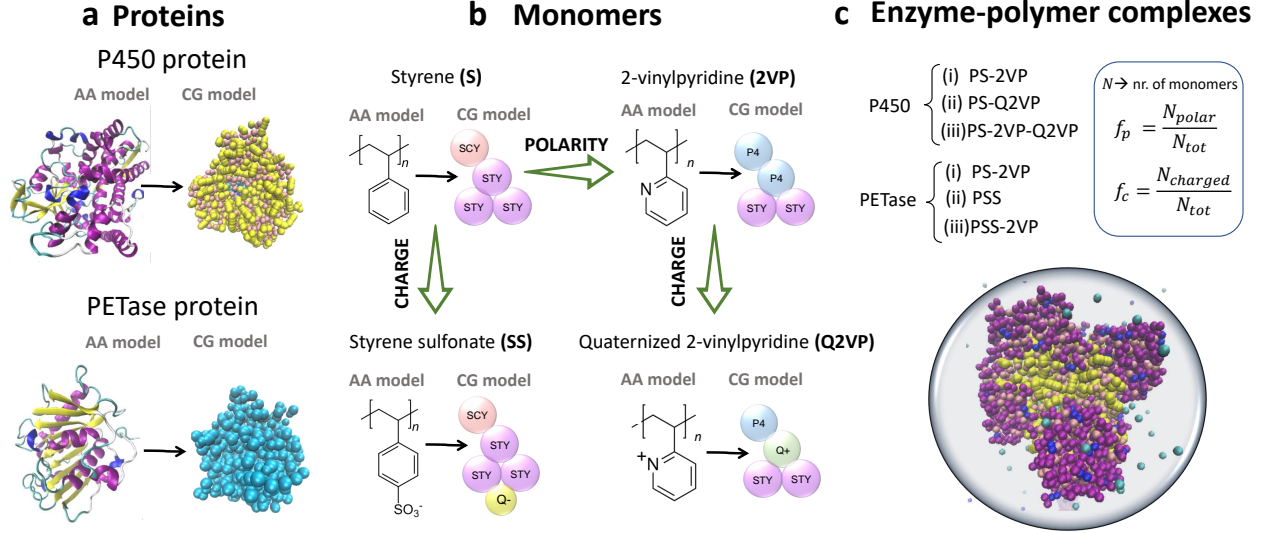$$f_c = \frac{N_{charged}}{N_{tot}}$$

.

Figure 1: Coarse-grained models and simulation setup. (a) Cytochrome P450 and PETase enzymes in both all-atom (AA) and Martini coarse-grained (CG) representations. (b) AA and CG Martini models of four monomers: styrene (S), 2-vinyl pyridine (2VP), styrene sulfonate (SS), and quaternized 2-vinyl pyridine (Q2VP). The heteropolymers considered here are obtained by randomly distributed these four monomers. (c) List of the enzyme-polystyrene-based complexes. The negatively charged (-15e) P450 co-assembly is tested with neutral polar PS-2VP (i), and positively charged (PS-Q2VP (ii), PS-2VP-Q2VP (iii)) random co-polymers; while the positively charged (+6e) PETase co-assembly is investigated with neutral polar PS-2VP (i), and negatively charged (PSS (ii), PSS-2VP (ii)) heteropolymers. The f_p and f_c fractions are tuned by altering the number of polar (N_{polar}) and charged ($N_{charged}$) monomers, respectively, over the total number of monomers ($N_{tot} = 60$) in one single polymer chain.

(Figure 1c). Table S1 and Table S2 in the Supporting Information (SI) document illustrate the details of polymer composition in all the study cases investigated. In the following paragraphs, after showing separately the results on polymer-polymer and polymer-enzyme self-assembly, we suggest the development of phase diagrams to guide the design of protein co-assembly by varying the polymer chemical composition.

Shape Conformation of Polymer-Polymer Self-Assembly

The self-assembling CG-MD simulations clearly show that the mechanism of complexes formation always occurs as a result of polymer-polymer and polymer-protein non bonded interactions. First, we demonstrate that modulation of the polar and charged monomer fraction, i.e., f_p and f_c parameters, respectively, alter the polymer-polymer aggregation strength which in turn drives the clustering process. Particularly, the enhancement of f_p, namely the progressive addition of neutral polar monomers (2VP) in the polystyrene homopolymer, does not substantially modify the velocity of clustering with fully non-polar polymers ($f_p = 0$), as shown in Figure S1 of the SI document. In both P450 and PETase enzyme solutions, the 20 initial chains completely self-aggregate in one single compact cluster in less than 1µs for the 70% of the tested cases. On the other hand, the insertion of charged monomers, i.e., the increase of f_c percentage, leads to a slow-down of the polymer self-assembly within the 2.5 µs simulated, that is particularly explicit in the case of $f_c = 40\%$ when just the 15% of the initial polymers creates one complex.

During the formation of enzyme-polymer complexes, cooperative supramolecular interactions (electrostatic, polar, and non-polar) emerge and define a hierarchy of mutual and self-affinities between polymers and proteins. The presence of enzymes indeed influences the kinetics of the polymer-polymer aggregation and the final equilibrium configuration. By comparing polymer self-assembly in systems with and without enzymes, we find that the presence of enzymes leads to more elongated aggregates than in enzyme-free systems (see Figure S2 in the SI document). The enzymes introduce nucleation sites for polymer-enzyme

8

bio-conjugates while limiting the degree of freedom for polymer-polymer self-interactions. In addition, the enzymes introduce directionality for polymer aggregation which is not present in the enzyme-free systems.

Beyond the dynamics of polymer-polymer self-aggregation, our simulation results highlight a distinction in cluster size and shape by tuning the polar and charged fractions (Figure 2a). The evaluation of the radius of gyration demonstrates that neutral polar heteropolymers aggregate in bigger clusters than the charged counterpart (see Figure S3 for PS-2VP and PS-Q2VP copolymers). In addition, the neutral polar chains, namely the PS-2VP polymers, tend to form more elongated complexes than either charged PS-Q2VP or PSS polymers. This last result is marked both in Figure 2b-c (Cytochrome P450 in solution) and Figure S4b-c (PETase in solution), where we report the maximum distance between two beads found in the biggest clusters. Going from fully hydrophobic $f_p = 0\%$ to completely polar homopolymers $f_p = 100\%$ we obtain an increase of the cluster elongation of roughly 50%, whereas the enhancement of charged monomer fraction, f_c, limits the assembly growth in a preferential direction, favoring aggregates with less polymers and a maximum distance between the beads equal to 15 nm ($f_c = 5\%$ in Figure 2c). In other words, the electrostatic repulsion between solvated charged copolymers prevents the polymer-polymer aggregation and hence the formation of long cluster chains which are instead promoted by polar-polar and hydrophobic interactions. Further confirmation of elongated clusters with a neutral polarity is given by the calculation of the asphericity parameter, which suggests how far the cluster is from a spherical shape. More details about the asphericity calculation are given in the Method section and reported in Figure S3 of the SI document.

The hydration and polarization effects indeed play a key role in the formation of protein-polymer complexes and their conformation. To assess the contributions from the water polarizability, we compared one system consisting of polarizable water particles with a second one of non-polarizable water particles, both systems containing one PETase protein and 20 PSS molecules (see Figure S5 in the SI document). We find that the bead-bead maxi-

9

mum separation distance (d) is larger within the polymer clusters of the system containing polarizable water beads than in the systems of non-polarizable water particles, namely, the aggregates are more elongated in polarizable water than in non-polarizable water. The polarizable water particles better hydrate the charged polymers than the non-polarizable water particles. This better hydration is responsible for limiting the self-aggregation among the charged polymers. We consider this point in greater detail in the discussion of the effect of added salt.
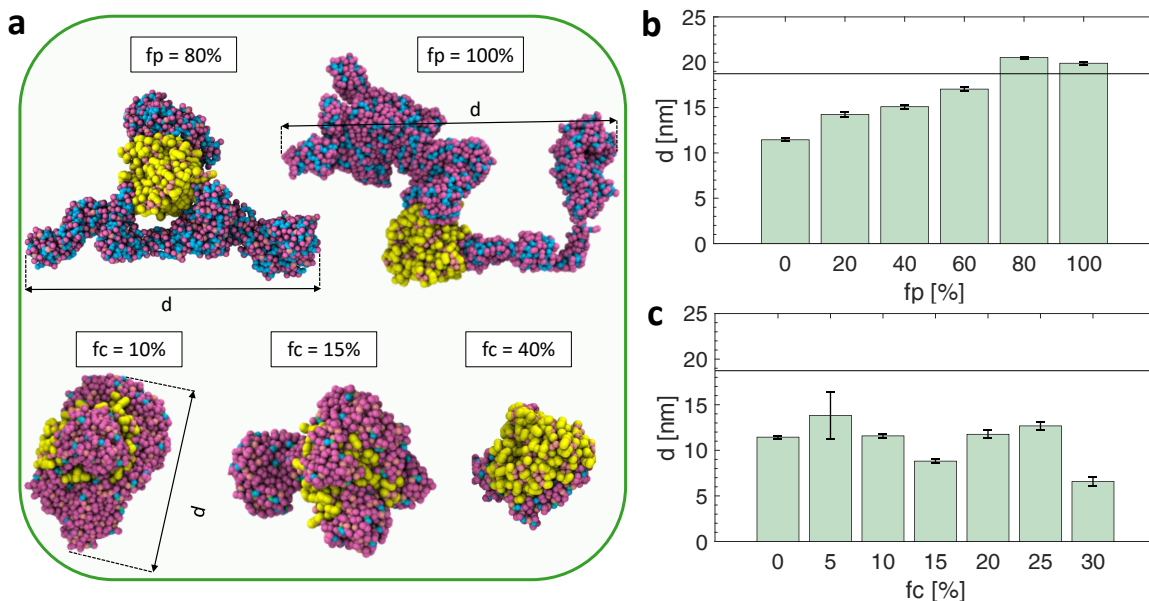

Figure 2: Polymer-P450 enzyme complexes. (a) MD-CG simulation snapshots of P450 with 20 neutral polar PS-2VP polymers (top) and 20 negative charged PS-Q2VP polymers (down) at various f_p and f_c values. (b-c) Bead-bead maximum distance inside the largest PS-2VP (b) and PS-Q2VP (c) polymer complexes as a function of the polar f_p and charge f_c percentage fractions.

Effect of Polymer Composition on the Enzyme-Polymer Self-Assembly

As already pointed out, the polar and charged nature of the heteropolymers not only influences the polymer self-aggregation but also affects the interactions with the enzyme, thereby modifying the balance of dominant mechanisms in the bio-conjugate formation. To understand the role of enzyme-polymer interactions, we computed the number of contacts

between the different random copolymers and the protein residues, namely polar, non-polar, and charged (see Figures 3a-b). A higher number of contacts, resulting from larger non-bonded pair interaction parameters reveal an improved probability to form bio-conjugates. Our results first highlight that the addition of polar 2VP monomers up to 20% enhances the polymer-protein aggregation points, as shown in Figure 3a. However, an increment of f_p above the 20% within the polymeric chain limits the number of contacts between PS-2VP heteropolymers and protein residues, in both Cytochrome P450 (Figure 3a) and PETase solutions (Figure S6). Analogous behavior is notable while using charged heteropolymers: although the effect of a small fraction of charges first promotes the formation of protein-polymer complexes, after reaching a maximum, the overall number of contacts decreases. In particular, the charged fraction, f_c, threshold is equal to 15% and 10% in Cytochrome P450 and PETase solutions, respectively (Figure 3b and Figure S5b). This analysis unveils that a progressive increase of hydrophilicity within the polymeric chain, obtained by introducing either polar or charged monomers, first promotes the single protein encapsulation, but then, above a specific threshold, the hydrophilic polymer nature favors the competitive interactions with the polar solvent, thereby limiting or even decreasing the enzyme-polymer contacts. In addition, by increasing the charge fraction, the number of contacts decreases due to the reduced number of adsorbed polymers on the protein surface.

It is worth noticing that the presence of charged monomers within the polymer chains, $i.e.$, when $f_c \neq 0$, determines higher enzyme-polymer contact points than those evaluated with neutral polar counterparts. As shown in Figures 3a and 3b, the average number of contacts per protein residue (light blue lines) becomes double passing from neutral polar heteropolymers (PS-2VP) to charged ones (PS-Q2VP). This result sheds light on the mechanisms of bio-conjugate formation. Specifically, for an equal number of hydrophobic monomers (like in the two cases $f_c = f_p = 15\%$), the polymer charged component contributes to weakening the polymer self-aggregation (see Figure S1) and the enzyme-polymer interactions prevail, leading to a consequential increase of the overall contact points per protein residue. For

example, the average number of contacts per protein residue goes from 2 to 5 when 15% of total monomers are converted from polar into charged. On the other hand, the intense self-affinity of neutral polar monomers encourages the formation of polymer aggregates that grow up from the contact sites on the enzyme surface (see the snapshots in Figure 2a and Figure 3a-3b). This behavior is observed below the f_c threshold, above which the role of solvent interactions and polymer repulsion strongly dominate, precluding a further enhancement of contact points within the bio-complexes.
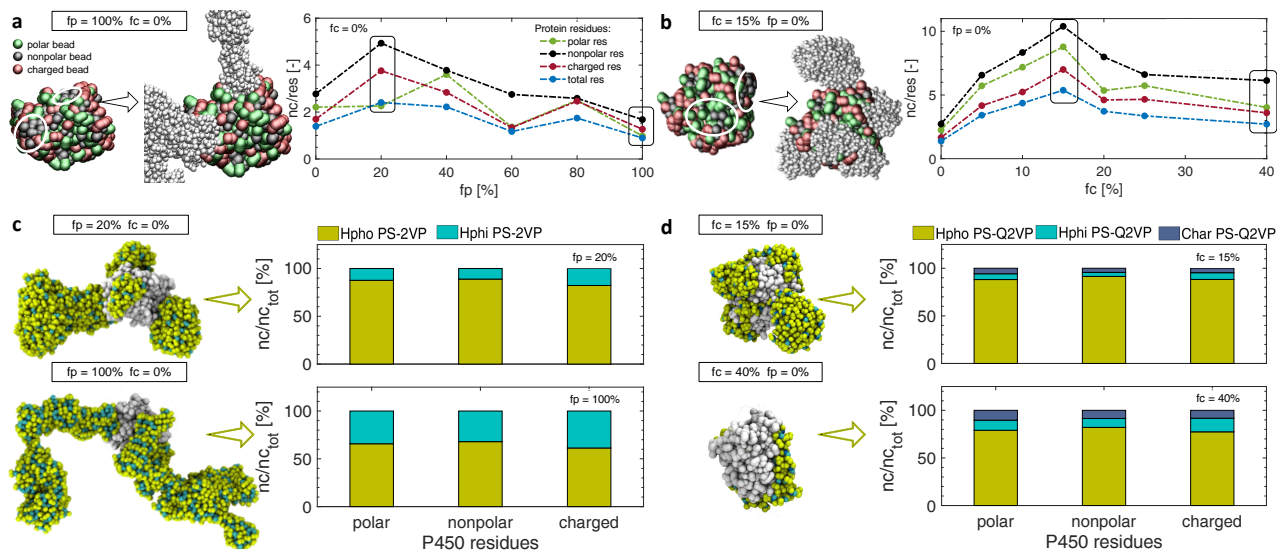

Figure 3: Polymer-P450 enzyme contacts. (a-b) Left side: CG-MD simulation snapshots of Cytochrome P450 before and after the polymer-enzyme self-aggregation in case of $f_p = 100\%, f_c = 0\%$ (a) and $f_c = 15\%, f_p = 0\%$ (b). Polar, non-polar, and charged beads in the P450 protein are depicted in green, black, and pink, respectively, and the non-polar regions where the polymer is adsorbed are indicated by a white circle; while the polymer beads are colored in white. Right side: Polymer-Cytochrome P450 number of contacts per protein residue, nc/res, as a function of polymer polar fraction, f_p (a) and polymer charge fraction, f_c (b). (c-d) Specific polymer adsorption quantified by the percentage of contacts (nc/nc_{tot}) between P450 residues (polar, non-polar, and charged) and hydrophilic (Hphi), hydrophobic (Hpho), and charged (Char) PS-2VP-Q2VP beads. Each bar accounts for the total number of contacts on a protein residue type; the percentages are represented using a color code according to the polymer bead type, namely, cyan, yellow, and blue correspond to hydrophilic, hydrophobic, and charged beads, respectively; P450 protein beads are colored in white. The number of protein residues is reported in Table S3 of the SI document.

Thorough cluster analysis and specifically the evaluation of the number of enzyme-

polymer contacts per residue unveils some key self-assembly mechanisms. Regardless of the polar and charged nature of polymers, and independently from the specific enzyme surface, the protein non-polar domains display always the highest number of contacts with the solvated heteropolymers (see the black lines in Figures 3a-b, Figure S6-S7). The simulation snapshots in Figure 3a-b, and Figure S8 qualitatively point out that the surface regions coated by polymers correspond to the non-polar domains. Figures 3c-d show the polymer beads types in contact with the protein residues (see Figure S8b of the SI document). The bar charts quantify the specific adsorption, namely, the percentage of specific polymer contacts (from hydrophobic and hydrophilic beads) on the specific protein residues (polar, nonpolar, and charged). These outcomes suggest that regardless of the polymer nature, the polymer-protein contacts occur mainly through the hydrophobic polymer beads (more than 60% of the contacts). In general, the number of binding contacts is a function of polymer nature, however, the type of beads involved in such cross-linking points are mainly hydrophobic. Each residue type binds the polymer beads in a similar way. This result reflects the polymer composition that results in the exposition of the protein residues to approximately the same number of hydrophobic and hydrophilic polymer beads. Fully hydrophobic polymers ($f_c = f_p = 0$) lead to a strong polymer-polymer self-aggregation, precluding a successful protein co-assembly. Therefore, a fraction of either charged or polar monomers is necessary for reaching an incisive protein coverage. The cooperative contribution of electrostatic and polar interactions modulate the supramolecular polymer-protein self-assembly.

Guidelines for Protein-Copolymer Coassembly Design

To give quantitative design rules for protein-copolymer co-assembly, we complete our study with a systematic screening in the polymer composition. Specifically, we investigate the bio-complex aggregation resulting from a simultaneous tuning of charge and polar fraction within our heteropolymers. The combination of the polymer-polymer and enzyme-polymer interactions on the self-assembly induces notable dissimilarities on the bio-complexes con-

figuration and co-assembly mode. The phase diagrams in Figures 4 and 5 outline the main results obtained in this combined analysis where the physical-chemistry nature of polymers is correlated with both the co-assembly efficiency and structure. Based on the maximum distance parameter d, previously described in the context of polymer self-assembly, and on the polymer-enzyme contacts, three types of co-assembly regimes can be distinguished:

- Membrane-like co-assembly: $d > 15.5$ nm and $\frac{nc}{res} < 2.2$ or $d > 18$ nm;

- Single protein encapsulation wrapping: $d < 15.5$ nm and $\frac{nc}{res} > 2.2$;

- Weak encapsulation: $d < 15.5$ nm and $\frac{nc}{res} < 2.2$.

First, a membrane-like co-assembly suggests the formation of a protein lattice in an extended polymer network, resembling an hydrogel structure. Accordingly, this co-assembly mode is defined in a regime of small protein-polymer contacts and elongated polymer assemblies. Second, the single protein encapsulation is characterized by a significant enzyme surface coverage by compact polymers. Consequentially, this type of bio-complexes is identified by a large number of contact points and a reduced size of polymer self-assemblies. Third, the weak encapsulation unveils the inefficient bio-complexes formation, described by very low polymer-enzyme contacts. More details are provided in the Method section.

The phase diagram in Figure 4 draws the main design rules to address and engineer the Cytochrome P450 co-assembly with polystyrene-based heteropolymers. In the region of low charge fraction, namely $f_c < 15\%$, the random substitution of styrene with charged Q2VP monomers reduces the polymer self-aggregation because of the electrostatic repulsion, and intensifies the nonbonded interactions with the P450 enzyme, thereby increasing the number of contact points and promoting the single protein encapsulation. However, as already emphasized, the excessive use of polar building blocks corresponding to $f_p > 20\%$, starts introducing a competitive affinity with both the polymers themselves and the surrounding polar solvent, leading to less intense protein-polymer interactions. This results in the formation of more elongated polymer chains with few contact points on P450 surface, mainly
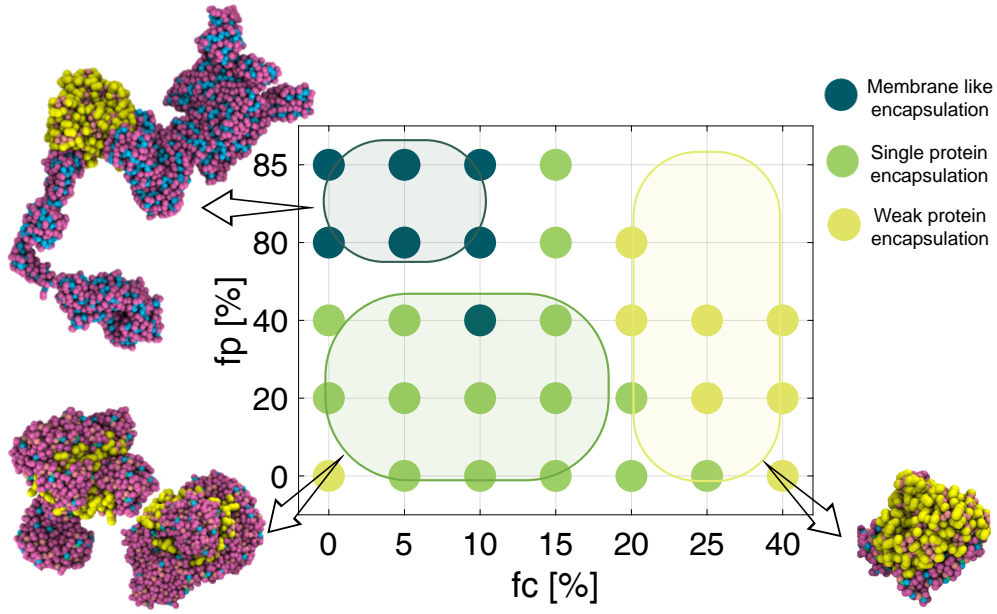
14

Figure 4: Phase diagram of polymer-P450 enzyme complexes. Tuning the polymer polar (f_p) and charge (f_c) fractions, three co-assembly modes of bio-complexes are identifiable: (i) the membrane-like co-assembly displayed with dark green points, (ii) the single protein encapsulation marked with light green points, and (iii) weak encapsulation depicted with yellow points. CG-MD snapshots are reported to clarify the overall shape and configuration of the bio-complexes into the three regimes.

concentrated on the non-polar residues, as discussed and proved before. For this reason, the top left side of the phase diagram in Figure 4 is predominantly characterized by a membrane-like co-assembly. Finally, for $f_p > 20\%$ and $f_c > 15\%$ the P450 phase diagram highlights a region of completely weak encapsulation. Here, the strong electrostatic repulsion due to the high charge fraction prevents the formation of self-aggregated polymer network crucial for a membrane-like co-assembly. Moreover, although single polymer chains adhere to the Cytochrome P450 surface creating several contacts with the enzyme, the polymer-polymer electrostatic repulsion together with the moderate collapsed configuration of a single PS-2VP-Q2VP polymer chain (see Figure 1b) inhibits a conspicuous protein coverage required to establishing a strong and robust single protein encapsulation.

The guidelines of PETase-copolymer co-assembly are summarized in Figure 5. First, we confirm that the non-polar PETase residues are the most covered by polymers as demonstrated by the highest number of contacts per non-polar PETase residue in Figures 5a-b and S9 in the SI document. Moreover, as pointed out in the previous paragraph, the low surface charge of this enzyme softens the effects of polymer charge fraction on the bio-complexes formation. The number of PETase-polymer contacts slightly varies for $f_c > 10\%$ as shown in Figure 5a-b, thereby preserving mostly the same bio-complex conformation, typical of a single protein encapsulation. However, although the protein surface coverage does not change significantly, the increase of the polymer charge fraction f_c leads to a higher percentage of electrostatic contribution in charged residue-charged polymer contacts, as demonstrated in the bar charts of Figure 5c and Figure S10. On the other hand, similarly to the P450 behavior, the increment of 2VP monomer fraction f_p favors the formation of elongated polymers which facilitates the network for membrane-like co-assembly (phase diagram in Figure 5d). Interestingly, the encapsulation of the PETase enzyme never shows strongly unfavorable conditions, as also confirmed by the phase diagram: here just a single point corresponding to $f_c = 30\%$ and $f_p = 70\%$ can be classified as a weak encapsulation mode. Such behavior can be explained by recalling the different conformation of Q2VP and SS monomers em-
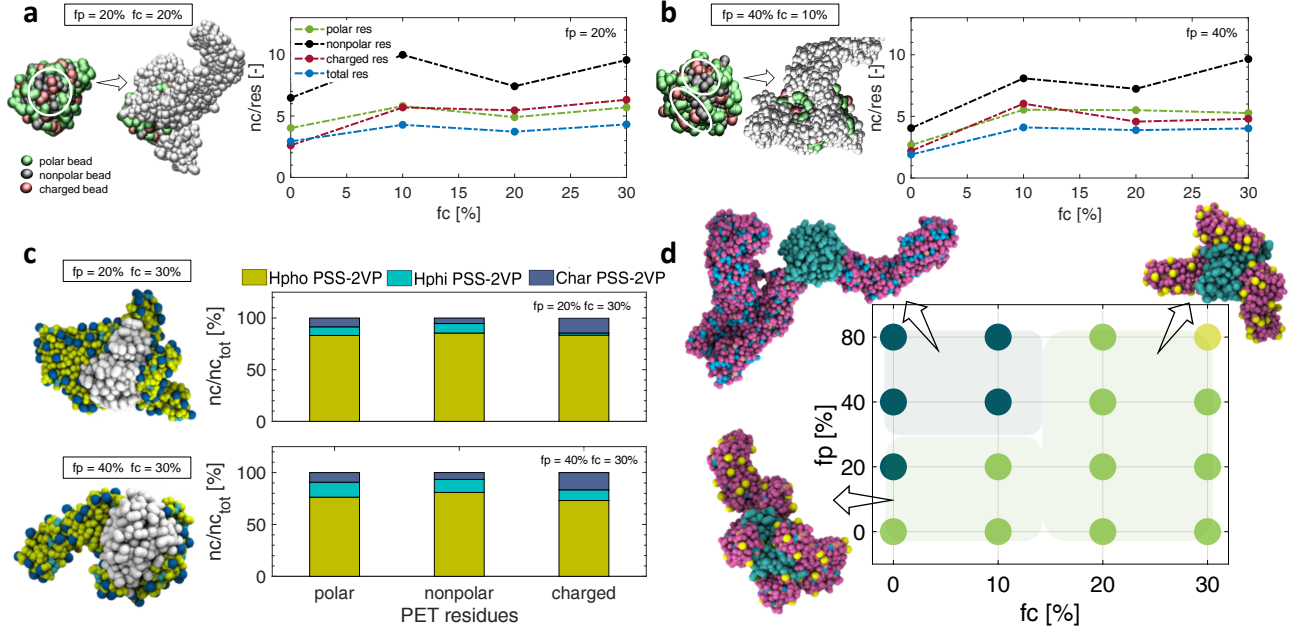
Figure 5: Polymer-PETase enzyme complexes. (a-b) Left: CG-MD simulation snapshots of PETase before and after the PSS-2VP-PETase self-aggregation. Two exemplary cases of PSS-2VP are selected: $f_p = 20\%$, $f_c = 20\%$ (a), and $f_p = 40\%$, $f_c = 10\%$ (b). Right: The polymer-PETase number of contacts per protein residue, nc/res, are plotted as a function of the polymer charge fraction, f_c. (c) Percentage of contacts (nc/nc$_{tot}$) between PETase enzyme residues (polar, non-polar, and charged) and hydrophilic (Hphi), hydrophobic (Hpho), and charged (Char) polymer beads. Hydrophilic, hydrophobic, and charged beads in the polymer chains are colored in cyan, yellow, and blue, respectively; while PETase enzyme beads are in white. d) Phase diagram of polymer-PETase complexes. The CG-MD snapshots illustrate the membrane-like co-assembly (dark green points) and single protein (light green points) encapsulation.

17

ployed in positive and negative polymer chains respectively. As illustrated in Figure 1b the chemical structure of the SS monomer is characterized by a charge bead well exposed to the solvent, while the positive charge in the counterpart monomer (Q2VP) is screened by the non-polar hydrocarbon beads. These contrasts in the chemical structure lead to a more solvated and extended configuration of PSS-2VP, than the Q2VP-based polymers, also when they are adsorbed on the protein surface. Consequently, the PSS polymers are involved in a larger number of contacts with the enzyme, favoring the overall coverage and the single protein encapsulation mode. In conclusion, the structural properties and the chemical/physical behavior of bio-conjugates lead to a more successful single protein encapsulation in PSS-2VP-PETase conjugates than the PS-2VP-Q2VP-P450 protein assemblies due to the more exposed charged groups of SS.

Finally, we enrich our analysis by investigating the self-assembly of PSS-2VP-PETase in 0.1 M NaCl solutions. The ionic correlations from the electrolyte induce interparticle long range interactions, affecting the polymer self-assembly.[37,38] We observe that the monovalent salt leads to more elongated protein-polymer aggregates than with no added salt (see Figures S11a-b and S12a). The increase of the elongation is more significant at low polymer charge fractions ($f_c < 20\%$) and is less important at polymer charge fractions higher than 30%. Our analysis suggests that the more elongated clusters result from the ionic correlations that promote a better polymer hydration even at low polymer charge fractions (see Figures S12b and S13). This phenomenon strongly influences the PETase-polymer phase diagram (see Figure S11c). Hence, at 0.1 M NaCl the membrane-like co-assembly region occurs at low polymer charge fractions ($f_c \lesssim 20$) for all the polar fractions. In contrast, at zero salt concentration the membrane-like structures are not formed at low charge and polar fractions ($f_c < 20\%$ and $f_p < 20\%$, see Figure 5d). Briefly, the enhancement of the polymer hydration alters the self-assembly mechanisms and increases the region of the membrane-like bio-conjugates.

CONCLUSIONS

The use of polymers to encapsulate proteins *via* self-assembly has led to interesting results in the last decades, suggesting a systematic use of enzymes in industrial applications. Here, we present a modeling-based design that provides quantitative guidelines for an efficient random copolymer preparation in line with the specific purpose of protein co-assembly. Specifically, we provide a systematic study where the Cytochrome P450 and PETase enzymes are solvated with polystyrene-based polymers in an aqueous solution. Protein co-assembly is then observed and analyzed exploring a variety of charged and polar fraction values within the polymeric chains.

First, our results demonstrate that tuning of the physical-chemistry nature of the random copolymers directs the trade-off between the polymer-polymer and polymer-protein interactions, thereby affecting the efficiency of co-assembly. Fully hydrophobic polymers, such as polystyrene, exhibit a fast tendency to polymer self-aggregate, thus depleting the non-bonded interactions with proteins. By introducing a percentage of neutral polar monomers (*i.e.*, 2VP) within the polymeric chain, we observe an enhancement of the enzyme-polymers contacts, whereas the dynamics of polymer-polymer self-aggregation remain fast. The protein coverage achieves a maximum value at $f_p = 20\%$; after this threshold, the increment of 2VP monomers favors the polymer self-aggregation and the solvent affinity, promoting more elongated structures which aggregate to the enzyme in a reduced number of contact points.

Similar shreds of evidence are found for bio-conjugates designed with charged polymers, namely positive PS-Q2VP and negative PSS polymers combined with Cytochrome P450 and PETase, respectively. Below specific charge fraction thresholds, *i.e.*, $f_c = 15\%$ in P450 and $f_c = 10\%$ in PETase solutions, the enzyme-polymer interactions dominate, leading to a high number of contact points. However, a notable increase in the charge fraction leads to a reduction of protein co-assembly efficiency. In fact, in such conditions, the electrostatic repulsion between the polymers together with the prominent hydration in a polar solvent limit both the polymer self-aggregation and their assembly with enzymes. These outcomes

reveal that a progressive increase of hydrophilicity obtained by handling with polar and charged monomers, facilitates the bio-conjugate formation up to a fixed charge threshold, after that the single protein encapsulation phenomenon is limited or even lowered.

Interestingly, the analysis of the polymer-enzyme contacts per residue gives some physical insights into the self-assembly mechanisms. Regardless of the protein sample considered, and irrespective of the specific physical-chemistry nature of the polymers, the number of contacts per residue is always higher in the protein non-polar domains. Moreover, the hydrophobic polymer beads are always the most active in the enzyme-polymer contacts. This suggests that the mechanisms of bio-complex formation are first driven by the hydrophobic interactions with polymers, thereby defining the most robust contact points in the bio-complexes.

Finally, we conclude our study by providing several phase diagrams that enable the rational design of both Cytochrome P450 and PETase co-assembly with random copolymers into various structures. In particular, a systematic screening of polystyrene-based polymer composition allow us to detect the bio-complex conformation regimes which span from a membrane-like co-assembly achieved with highly polar neutral polymers to single protein encapsulation typical for low neutral polar and moderate charged monomer fractions. Lastly, we show that the presence of monovalent salt in solution strongly influences the self-assemby mechanisms and the structure of the polymer-protein bioconjugates. In the phase diagram, the salt ions enlarge the region where the membrane-like structures are formed.

METHODS

The enzyme-polymer self-assembly is simulated with a top-down Coarse-Grained Molecular Dynamics (CG-MD) approach. Specifically, we adopt the Martini force-field,[26,27] which relies on an effective four-to-one mapping scheme, to construct the CG model of both proteins (Figure 1 a) and polystyrene-based random copolymers (Figures 1 b-c).

The crystal structures of Cytochrome P450 and PETase enzyme are downloaded from

the Protein Data Bank (PDB) with PDB code ID 1BU7[28] and I6EQE[31] respectively. The AA model of each protein is coarse-grained using the scripts martinize.py,[36] including the ElNeDyn elastic network that allows changes in the orientation of the secondary elements while keeping the secondary structure of the protein motifs.[39] The CG parametrization of the HEME cofactor within the Cytochrome P450 relies on Reference.[40] Therefore, both the mapping scheme and the topology of proteins are set-up according to the Martini force field parameters.

The random copolymers considered in our self-assembly simulations are built by utilizing four types of monomers, as illustrated in Figure 1b. The hydrophobic building blocks are represented by styrene (s) monomers, whose CG model, including mapping and bond interactions, was developed by Rossi et $al.$[41] Specifically the SCY and STY bead types are used to model the $CH-CH_2$ and the aromatic ring, respectively. Then, the polarity is taken into account by coarse-graining the 2-vinyl pyridine (2VP) monomer as previously implemented by Jiménez-Ángeles et $al.$[32] who replaced two non-polar beads in the styrene with P4 bead type. Finally, the contribution of electrostatic interactions in the self-assembly mechanisms is counted by introducing the styrene sulfonate (SS) and the quaternized 2-vinyl pyridine (Q2VP) monomers. Specifically, the negatively charged sulfonate group which is bound to the phenyl ring (Figure 1b (SS) monomer) is modeled with an extra Qa CG bead type, which relies on hydrogen-bond acceptor properties and bears a negative net charge of $z = -1e$;[42] on the other hand, the CG model of Q2VP is based on the same mapping of 2VP monomer, but replacing the neutral polar bead P4 with a positive bead type Qd, which holds a net charge of $z = +1e$.[32] It is worth noticing that, the complete set of the nonbonded parameters in the CG models reported in Figure 1 corresponds to the standard bead type classification in the Martini force field. The random co-polymers simulated here are constituted by sixty total monomers each, namely $N_{tot} = 60 = N_s + N_{2vp} + N_{q2vp} + N_{ss}$, where the number of styrene (N_s), 2-vinyl pyridine (N_{2vp}), quaternized 2-vinyl pyridine (N_{q2vp}), and styrene-sulfonate (N_{ss}) monomers are tuned and randomly distributed inside the chain. As a

consequence, we can define the polar fraction of the heteropolymer chain as $f_p = N_{polar}/N_{tot}$, where N_{polar} is the number of neutral polar monomers (N_{2vp}), whereas the charge fraction as $f_c = N_{charged}/N_{tot}$, with $N_{charged}$ equal to either N_{q2vp} or N_{ss} (see Figure 1c). In a fully neutral hydrophilic homopolymer $N_{tot} = N_{2vp}$ implying $f_p = 1$, whereas $N_{tot} = Ns$ and $f_p = 0$ in a fully neutral hydrophobic homopolymer.

The protein-polymers self-assembly simulations were carried out in aqueous solution using a simulation box containing 20 polymer molecules, 1 single protein and polarizable water particles, according to the Martini parametrization.[34] The number of counterions were adjusted accordingly with the protein and polymer charge fraction fc. In particular, six negative and fifteen positively charged beads were added to neutralize the net charge on PETase (+6e) and P450 (-15e), respectively and the remaining counterions were included in the box to balance the charged polymers. The simulation box dimensions are $L_x = 20$ nm, $L_y = 20$ nm, and $L_z = 20$ nm in the x-, y-, and z-directions, respectively. Our simulation protocol consists of a 50 ns of equilibration run to thermalize the system at p = 1 atm and T = 300 K; in this step, we used the velocity re-scale thermostat[43] ($\tau_T = 2$ ps) and Berendsen barostat[44] ($\tau_p = 12$ ps). During the production runs, lasting 2.5 μs, we applied the velocity-rescaling thermostat and the Parrinello-Rahman barostat,[45] still maintaining p = 1 atm and T = 300 K. A time-step of 15 fs is used to integrate Newton's equations of motion. Short-range interactions are truncated at 1.2 nm, and long-range electrostatic interactions are computed using the PME algorithm. Three-dimensional periodic boundary conditions are applied. The simulations are performed using the open-source code GROMACS 2016.3.[46]

All the post-processing analyses, including the time evolution of clusters, the evaluation of the cluster size, shape, and finally the enzyme-polymer number of contacts are computed by combining the GROMACS post-processing tools and in-house codes. To calculate the number of contacts we selected a cut-off distance of 0.6 nm. A cut-off distance smaller than 0.45 nm (the mean bead diameter in the Martini model) is not enough to capture the bead-bead contacts whereas a cut-off distance larger than 0.7 nm would include contacts beyond

the first neighbors. The convergence of the self-assembled polymer-polymer and polymer-protein structures is discussed in Figure S1 in the Supporting Information. In particular, after obtaining the bead positions inside the clusters from the MD trajectories, we computed the bead-bead maximum distances, d, and the radius of gyration, Rg, of the biggest cluster in the last step of the self-assembly simulation. Rg is defined as the first invariant of the gyration tensor S, namely:

$$Rg^2 = TrS = \lambda_1 + \lambda_2 + \lambda_3 \tag{1}$$

Moreover, we characterized the cluster shape by estimating the asphericity parameter, which is defined as the second invariant of the gyration tensor S, namely:

$$As = \frac{3}{2}\frac{Tr\hat{S}^2}{(TrS)^2} = 1 - 3\frac{\lambda_1\lambda_2 + \lambda_1\lambda_3 + \lambda_2\lambda_3}{(\lambda_1 + \lambda_2 + \lambda_3)^2} \tag{2}$$

where λ_1, λ_2, λ_3, are the eigenvalues of the gyration tensor, S, of the cluster. As ranges from 0 to 1 corresponding to a spherical shape and an infinite rod, respectively.

The average number of contacts per single residue (nc/res) was computed first by counting during the last 800 ns of the trajectory the total number of contacts between polymer beads and polar, non-polar, and charged protein residues. Then we divided the total contacts by the corresponding number of residues, considering the distribution of protein residues on the surface. Once we obtained the average number of contacts per residue, we evaluated the contribution coming from the hydrophilic, hydrophobic, and charged nature of polymer beads (nc/nc$_{tot}$).

For completing the bio-complex phase diagrams we have employed the maximum distance, d, within the polymer self-assembly and the number of contacts per protein residue, $\frac{nc}{res}$ namely:

- Membrane-like co-assembly: $d > 15.5$ nm and $\frac{nc}{res} < 2.2$ or $d > 18$ nm;

- Single protein encapsulation: $d < 15.5$ nm and $\frac{nc}{res} > 2.2$;

- Weak encapsulation: $d < 15.5$ nm and $\frac{nc}{res} < 2.2$.

ACKNOWLEDGEMENTS

ASSOCIATED CONTENT

Supporting Information

The Supporting Information is available free of charge at https://pubs.acs.org/

Details of the polymer composition, polymer-polymer cluster analysis, quantification of the polymer-enzyme assemblies, analysis of the biggest polymer clusters, PETase enzyme-polymer complexes, polarizable and non-polarizable water models in polymer-protein assembly, analysis of cytochrom P450 and PETase by residues, number of contacts in polymer-enzyme assemblies at different polymer compositions, influence of the addition of NaCl on the polymer-enzyme assembly (PDF)

REFERENCES

(1) Dunn, P. J. The Importance of Green Chemistry in Process Research and Development. *Chemical Society Reviews* **2012**, *41*, 1452–1461.

(2) Fang, X.; Kalathil, S.; Reisner, E. Semi-Biological Approaches to Solar-to-Chemical Conversion. *Chemical Society Reviews* **2020**, *49*, 4926–4952.

(3) Chen, Y.; Li, P.; Zhou, J.; Buru, C. T.; Đorđević, L.; Li, P.; Zhang, X.; Cetin, M. M.; Stoddart, J. F.; Stupp, S. I.; Wasielewski, M. R.; Farha, O. K. Integration of Enzymes and Photosensitizers in a Hierarchical Mesoporous Metal–Organic Framework for Light-Driven CO_2 Reduction. *Journal of the American Chemical Society* **2020**, *142*, 1768–1773.

(4) Arnold, F. H. Directed Evolution: Bringing New Chemistry to Life. *Angewandte Chemie International Edition* **2018**, *57*, 4143–4148.

(5) Chen, Y.; Li, P.; Modica, J. A.; Drout, R. J.; Farha, O. K. Acid-Resistant Mesoporous Metal–Organic Framework toward Oral Insulin Delivery: Protein Encapsulation, Protection, and Release. *Journal of the American Chemical Society* **2018**, *140*, 5678–5681.

(6) Cai, J.; Sweeney, A. M. The Proof is in the Pidan: Generalizing Proteins as Patchy Particles. *ACS Central Science* **2018**, *4*, 840–853.

(7) Nicolai, T.; Durand, D. Protein Aggregation and Gel Formation Studied with Scattering Methods and Computer Simulations. *Current Opinion in Colloid & Interface Science* **2007**, *12*, 23–28.

(8) Gnan, N.; Sciortino, F.; Zaccarelli, E. In *Protein Self-Assembly: Methods and Protocols*; McManus, J. J., Ed.; Springer New York: New York, NY, 2019; pp 187–208.

(9) Chen, Y.; Jiménez-Ángeles, F.; Qiao, B.; Krzyaniak, M. D.; Sha, F.; Kato, S.; Gong, X.; Buru, C. T.; Chen, Z.; Zhang, X.; Gianneschi, N. C.; Wasielewski, M. R.; Olvera de la Cruz, M.; Farha, O. K. Insights into the Enhanced Catalytic Activity of Cytochrome c When Encapsulated in a Metal–Organic Framework. *Journal of the American Chemical Society* **2020**, *142*, 18576–18582.

(10) Wu, X.; Yue, H.; Zhang, Z.; Gao, X.; Li, X.; Wang, L.; Cao, Y.; Hou, M.; An, H.; Zhang, L.; Li, S.; Ma, J.; Lin, H.; Fu, Y.; Gu, H.; Lou, W.; Wei, W.; Zare, R. N.; Ge, J. Packaging and Delivering Enzymes by Amorphous Metal-Organic Frameworks. *Nature Communications* **2019**, *10*, 1–8.

(11) Panganiban, B.; Qiao, B.; Jiang, T.; DelRe, C.; Obadia, M. M.; Nguyen, T. D.; Smith, A. A.; Hall, A.; Sit, I.; Crosby, M. G.; Dennis, P. B.; Drockenmuller, E.; Olvera de la Cruz, M.; Xu, T. Random Heteropolymers Preserve Protein Function in Foreign Environments. *Science* **2018**, *359*, 1239–1243.

(12) Lyu, F.; Zhang, Y.; Zare, R. N.; Ge, J.; Liu, Z. One-Pot Synthesis of Protein-Embedded Metal–Organic Frameworks with Enhanced Biological Activities. *Nano Letters* **2014**, *14*, 5761–5765.

(13) Liu, Y.; Nevanen, T. K.; Paananen, A.; Kempe, K.; Wilson, P.; Johansson, L.-S.; Joensuu, J. J.; Linder, M. B.; Haddleton, D. M.; Milani, R. Self-Assembling Protein-Polymer Bioconjugates for Surfaces with Antifouling Features and Low Nonspecific Binding. *ACS Appl Mater Interfaces* **2019**, 3599–3608.

(14) Theodorou, A.; Liarou, E.; Haddleton, D. M.; Stavrakaki, I. G.; Skordalidis, P.; Whitfield, R.; Anastasaki, A.; Velonia, K. Protein-Polymer Bioconjugates *via* a Versatile Oxygen Tolerant Photoinduced Controlled Radical Polymerization Approach. *Nature Communications* **2020**, *11*, 1–11.

(15) Qin, G.; Glassman, M. J.; Lam, C. N.; Chang, D.; Schaible, E.; Hexemer, A.; Olsen, B. D. Topological Effects on Globular Protein-ELP Fusion Block Copolymer Self-Assembly. *Advanced Functional Materials* **2015**, *25*, 729–738.

(16) Chang, D.; Lam, C. N.; Tang, S.; Olsen, B. D. Effect of Polymer Chemistry on Globular Protein–Polymer Block Copolymer Self-Assembly. *Polymer Chemistry* **2014**, *5*, 4884–4895.

(17) Obermeyer, A. C.; Olsen, B. D. Synthesis and Application of Protein-Containing Block Copolymers. *ACS Macro Letters* **2015**, *4*, 101–110.

(18) Chang, D.; Huang, A.; Olsen, B. D. Kinetic Effects on Self-Assembly and Function of Protein–Polymer Bioconjugates in Thin Films Prepared by Flow Coating. *Macromolecular Rapid Communications* **2017**, *38*, 1600449.

(19) Huang, A.; Paloni, J. M.; Wang, A.; Obermeyer, A. C.; Sureka, H. V.; Yao, H.; Olsen, B. D. Predicting Protein–Polymer Block Copolymer Self-Assembly from Protein Properties. *Biomacromolecules* **2019**, *20*, 3713–3723.

(20) Zhang, L.; Bailey, J. B.; Subramanian, R. H.; Groisman, A.; Tezcan, F. A. Hyperexpandable, Self-Healing Macromolecular Crystals with Integrated Polymer Networks. *Nature* **2018**, *557*, 86–91.

(21) Korpi, A.; Skumial, P.; Kostiainen, M. A. Thermally Induced Reversible Self-Assembly of Apoferritin–Block Copolymer Complexes. *Macromolecular Rapid Communications* **2019**, *40*, 1900308.

(22) Wang, J.; Waltmann, C.; Umana-Kossio, H.; Olvera de la Cruz, M.; Torkelson, J. M. Heterogeneous Charged Complexes of Random Copolymers for the Segregation of Organic Molecules. *ACS Central Science* **2021**, *7*, 882–891.

(23) Li, Y.; Qiao, B.; Olvera de la Cruz, M. Protein Surface Printer for Exploring Protein Domains. *Journal of Chemical Information and Modeling* **2020**, *60*, 5255–5264.

(24) Qiao, B.; Jiménez-Ángeles, F.; Nguyen, T. D.; de la Cruz, M. O. Water Follows Polar and Nonpolar Protein Surface Domains. *Proceedings of the National Academy of Sciences* **2019**, *116*, 19274–19281.

(25) Nguyen, T. D.; Qiao, B.; de la Cruz, M. O. Efficient Encapsulation of Proteins with

Random Copolymers. *Proceedings of the National Academy of Sciences* **2018**, *115*, 6578–6583.

(26) Marrink, S. J.; Risselada, H. J.; Yefimov, S.; Tieleman, D. P.; De Vries, A. H. The MAR-TINI Force Field: Coarse Grained Model for Biomolecular Simulations. *The Journal of Physical Chemistry B* **2007**, *111*, 7812–7824.

(27) Marrink, S. J.; Tieleman, D. P. Perspective on the Martini Model. *Chemical Society Reviews* **2013**, *42*, 6801–6822.

(28) Sevrioukova, I. F.; Li, H.; Zhang, H.; Peterson, J. A.; Poulos, T. L. Structure of a Cy-tochrome P450–Redox Partner Electron-Transfer Complex. *Proceedings of the National Academy of Sciences* **1999**, *96*, 1863–1868.

(29) Guengerich, F. P. Cytochrome P450 and Chemical Toxicology. *Chemical Research in Toxicology* **2008**, *21*, 70–83.

(30) Ortiz de Montellano, P. R. Hydrocarbon Hydroxylation by Cytochrome P450 Enzymes. *Chemical Reviews* **2010**, *110*, 932–948.

(31) Austin, H. P.; Allen, M. D.; Donohoe, B. S.; Rorrer, N. A.; Kearns, F. L.; Silveira R. L.; Pollard, B. C.; Dominick, G.; Duman, R.; Omari, K. E.; Mykhaylyk, V.; Wagner, A.; Michener, W. E.; Amore, A.; Skaf, M. S.; Crowley, M. F.; Thorne, A. W.; Johnson Ch. W.; Woodcock H. L.; McGeehan, J. E; et al. Characterization and Engineering of a Plastic-Degrading Aromatic Polyesterase. *Proceedings of the National Academy of Sciences* **2018**, *115*, E4350–E4357 .

(32) Jiménez-Ángeles, F.; Kwon, H.-K.; Sadman, K.; Wu, T.; Shull, K. R.; Olvera de la Cruz, M. Self-Assembly of Charge-Containing Copolymers at the Liquid–Liquid Inter-face. *ACS Central Science* **2019**, *5*, 688–699.

(33) Jiménez-Ángeles, F.; Harmon, K. J.; Nguyen, T. D.; Fenter, P.; Olvera de la Cruz, M. Nonreciprocal Interactions Induced by Water in Confinement. *Physical Review Research* **2020**, *2*, 043244.

(34) Yesylevskyy, S. O.; Schäfer, L. V.; Sengupta, D.; Marrink, S. J. Polarizable Water Model for the Coarse-Grained MARTINI Force Field. *PLoS Comput Biol* **2010**, *6*, e1000810.

(35) Wang, W.; Narain, R.; Zeng, H. Hydrogels. In *Polymer Science and Nanotechnology: Fundamentals and Applications*; 1st Edition; Elsevier, 2020; pp 203–244 .

(36) Monticelli, L.; Kandasamy, S. K.; Periole, X.; Larson, R. G.; Tieleman, D. P.; Marrink, S.-J. The MARTINI Coarse-Grained Force Field: Extension to Proteins. *Journal of Chemical Theory and Computation* **2008**, *5*, 819–834.

(37) Li, Y.; Girard, M.; Shen, M.; Millan, J. A.; De La Cruz, M. O. Strong Attractions and Repulsions Mediated by Monovalent Salts. *Proceedings of the National Academy of Sciences* **2017**, *114*, 11838–11843.

(38) Kewalramani, S.; Guerrero-García, G. I.; Moreau, L. M.; Zwanikken, J. W.; Mirkin, C. A.; Olvera de la Cruz, M.; Bedzyk, M. J. Electrolyte-Mediated Assembly of Charged Nanoparticles. *ACS Central Science* **2016**, *2*, 219–224.

(39) Periole, X.; Cavalli, M.; Marrink, S.-J.; Ceruso, M. A. Combining an Elastic Network with a Coarse-Grained Molecular Force Field: Structure, Dynamics, and Intermolecular Recognition. *Journal of Chemical Theory and Computation* **2009**, *5*, 2531–2543.

(40) de Jong, D. H.; Liguori, N.; van den Berg, T.; Arnarez, C.; Periole, X.; Marrink, S. J. Atomistic and Coarse Grain Topologies for the Cofactors Associated with the Photosystem II Core Complex. *The Journal of Physical Chemistry B* **2015**, *119*, 7791–7803.

(41) Rossi, G.; Monticelli, L.; Puisto, S. R.; Vattulainen, I.; Ala-Nissila, T. Coarse-Graining

Polymers with the MARTINI Force-Field: Polystyrene as a Benchmark Case. *Soft Matter* **2011**, *7*, 698–708.

(42) Vögele, M.; Holm, C.; Smiatek, J. Coarse-Grained Simulations of Poly-electrolyte Complexes: MARTINI Models for Poly(Styrene Sulfonate) and Poly(Diallyldimethylammonium). *The Journal of Chemical Physics* **2015**, *143*, 243151 .

(43) Bussi, G.; Donadio, D.; Parrinello, M. Canonical Sampling through Velocity Rescaling. *The Journal of Chemical Physics* **2007**, *126*, 014101.

(44) Berendsen, H. J.; Postma, J. v.; van Gunsteren, W. F.; DiNola, A.; Haak, J. R. Molec-ular Dynamics with Coupling to an External Bath. *The Journal of Chemical Physics* **1984**, *81*, 3684–3690.

(45) Parrinello, M.; Rahman, A. Polymorphic Transitions in Single Crystals: A New Molec-ular Dynamics Method. *Journal of Applied Physics* **1981**, *52*, 7182–7190.

(46) Abraham, M. J.; Murtola, T.; Schulz, R.; Páll, S.; Smith, J. C.; Hess, B.; Lindahl, E. GROMACS: High Performance Molecular Simulations through Multi-Level Parallelism from Laptops to Supercomputers. *SoftwareX* **2015**, *1*, 19–25.

Graphical TOC Entry

Random copolymers

PROTEIN ENCAPSULATION

Protein